JOURNAL OF VIROLOGY, Sept. 1997, p. 6765–6776 Vol. 71, No. 9
0022-538X/97/$04.00+0

Effects of Nucleocapsid Mutations on Human Immunodeficiency Virus Assembly and RNA Encapsidation

YAQIANG ZHANG AND ERIC BARKLIS*

Vollum Institute for Advanced Biomedical Research and Department of Molecular Microbiology and Immunology, Oregon Health Sciences University, Portland, Oregon 97201-3098

Received 3 December 1996/Accepted 20 May 1997

The human immunodeficiency virus (HIV) $Pr55^{Gag}$ precursor proteins direct virus particle assembly. While Gag-Gag protein interactions which affect HIV assembly occur in the capsid (CA) domain of $Pr55^{Gag}$, the nucleocapsid (NC) domain, which functions in viral RNA encapsidation, also appears to participate in virus assembly. In order to dissect the roles of the NC domain and the p6 domain, the C-terminal Gag protein domain, we examined the effects of NC and p6 mutations on virus assembly and RNA encapsidation. In our experimental system, the p6 domain did not appear to affect virus release efficiency but p6 deletions and truncations reduced the specificity of genomic HIV-1 RNA encapsidation. Mutations in the nucleocapsid region reduced particle release, especially when the p2 interdomain peptide or the amino-terminal portion of the NC region was mutated, and NC mutations also reduced both the specificity and the efficiency of HIV-1 RNA encapsidation. These results implicated a linkage between RNA encapsidation and virus particle assembly or release. However, we found that the mutant ApoMTRB, in which the nucleocapsid and p6 domains of HIV-1 $Pr55^{Gag}$ were replaced with the *Bacillus subtilis* MtrB protein domain, released particles efficiently but packaged no detectable RNA. These results suggest that, for the purposes of virus-like particle assembly and release, NC can be replaced by a protein that does not appear to encapsidate RNA.

The human immunodeficiency virus type 1 (HIV-1) proviral DNA encodes three major genes, *gag*, *pol*, and *env*, as well as a number of accessory genes. Expression from the proviral long terminal repeat promoters ultimately leads to the transcription of spliced and full-length viral RNAs. The viral Gag protein is translated from the full-length messenger RNA and is synthesized initially as the polyprotein precursor $Pr55^{Gag}$ (9, 55, 65). Cellular expression of $Pr55^{Gag}$ has been shown to result in the formation of virus-like particles (18, 22, 35, 44, 58, 59). During or shortly after budding, $Pr55^{Gag}$ proteins are cleaved by the protease (PR) encoded by the *pol* open reading frame (ORF), which yields a processing intermediate (p41) and the mature Gag proteins matrix (MA), capsid (CA), nucleocapsid (NC), and p6 (26, 39, 46, 51, 55). The interdomain peptides p2 (between CA and NC) and p1 (between NC and p6) also are generated via this event. Coincident with processing, HIV particles take on new morphologies, acquiring an electron-dense conical or cylindrical core, and become more sensitive to disruption by nonionic detergents.

Several studies have indicated that protein-protein interactions required for wild-type (wt) levels of $Pr55^{Gag}$ self-assembly into virus particles occur in the CA region (53, 60, 62, 66, 68), while numerous studies have implicated HIV NC in the incorporation of HIV RNA into virus particles (1, 3, 11, 16, 19, 31, 45, 71). This is not surprising, since the nucleocapsid domain consists of an N-terminal, positively charged region, a proximal Cys-His finger motif, an interfinger region, a distal Cys-His finger motif, and a C-terminal section (28, 47, 50, 64). Nevertheless, while experiments have shown that NC contributes to the specificity of RNA encapsidation (7, 71), the influence of other Gag domains on this process remains unclear. Also unclear is the relationship between RNA encapsidation and HIV particle assembly. Recent findings have indicated that NC and the p2 and p1 interdomain regions define important assembly determinants (8, 10, 38). These regions may act directly by mediating critical Gag-Gag contacts or Gag protein interactions with cellular components. Alternatively, NC might exert its effect on assembly via its association with the capsid domain or with RNA, as has been observed in vitro (8).

To study the effects of the p2, NC, p1, and p6 domains of HIV-1 on virus assembly and RNA encapsidation, we have examined a series of C-terminal *gag* mutations in protease-minus (PR^-) and wt contexts. In our experimental system, we found that PR^- constructs were released more efficiently than the wt and that p1 and p6 mutations were neutral with regard to particle release. In contrast, other amino-terminal mutations, especially those in p2 or near the N terminus of NC, produced Pr^{Gag} proteins that were deficient in virus particle release. Additionally, two types of effects on encapsidation were observed: p2 and NC mutant particles packaged low levels of RNA and p1 and p6 mutants incorporated abnormally high levels of spliced viral RNAs, indicating a loss of encapsidation specificity. We also characterized a mutant, ApoMTRB, in which the HIV p1, NC, p2, and p6 domains were replaced with the tryptophan leader RNA binding protein encoded by the *Bacillus subtilis mtrB* gene (49). While ApoMTRB proteins efficiently assembled virus-like particles, the particles contained no detectable incorporation of spliced or unspliced viral RNA. Assuming that spliced RNA accurately assesses nonspecific RNA encapsidation, our results suggest that the assembly function of HIV-1 NC can be replaced by a protein that does not encapsidate RNA.

MATERIALS AND METHODS

Recombinant constructs. All the NC and p6 mutants were created from the parental wt construct HIVgpt (52, 66, 67), which is based on the HIV HXB2 strain (17), and the locations of all the mutations in this paper are numbered according to the numbering system of the proviral DNA sequence of HIV HXB2. HIVgpt uses the simian virus 40 origin of replication and early promoter to express the drug resistance guanosine phosphoribosyltransferase (*gpt*) (48) gene in place of the *env* coding sequence, while other viral genes remain intact.

* Corresponding author. Phone: (503) 494-8098. Fax: (503) 494-6862. E-mail: barklis@ohsu.edu.

Expression of HIVgpt in Cos7 cells results in the production of noninfectious (*env*-minus) but otherwise normal virus particles. The construct 2498T has an *Hpa*I linker insertion at the *Hin*dIII site at nucleotide (nt) 2498 of the HIV HXB2 proviral DNA sequence, stopping all three ORFs; it expresses wt Gag but produces immature virions, since *pol* gene products are not expressed. HIVgpt A15 (1, 66, 67, 71) is a construct in which the first two cysteine residues of the C-terminal NC Cys-His motif were mutated to tyrosine (1). Two other mutants, *Apa*I and *Bgl*II, possess linker insertions at nt 2010 and 2096, respectively, and have been described previously (66). The newly created ApoTE, MunTE, TARK, and TAM constructs cause the *gag* ORF to terminate at different positions in p2 or NC and eliminate *pol* ORF expression. The mutant sequences are as follows, where the 5′ and 3′ proviral nucleotide numbers are provided, wt HIV sequences are in normal type, oligonucleotides are in boldface type, and the termination codons are underlined: ApoTE, 5′ ACA **AAT TGA CCC GGG TCA** ATT C 3′ (nt 1899 to 1906); TAM, 5′ ACA **AAT TCA GCT ACC ATA ATG TGA CTG GA**A TTC 3′ (nt 1899 to 1906); TARK, 5′ ACA **AAT TCT GCT ACC ATC ATG ATG CAG AGA GGC AAT TTT AGG AAC CAA AGA AAG TAG** AAT TC 3′ (nt 1899 to 1906); and MunTE, 5′ TGT TTC **AAT TGA CCC GGG TC**A ATT G 3′ (nt 1962 to 1972). Another mutant, ApoMTRB, is one in which the HIV-1 NC and p6 domains have been replaced by the *B. subtilis trp* leader RNA binding protein encoded by the methyltryptophan resistance (*mtrB*) locus (49). The ApoMTRB DNA junction sequence starting at HIV-1 proviral nt 1899 is 5′ ACA **AAT TCC GGG CTG CAG GAA TTA ATT** *CAA AAG CAT TCA* 3′, where the HIV sequence is in normal type, the linker sequence is in boldface type, and the *mtrB* sequence, which starts at *mtrB* codon 3, is in italic type. In addition to the above-named mutations, three internal deletions were created in the HIV-1 NC coding region. ΔMun deletes NC sequences from the *Mun*I site at nt 1968 to the *Rsa*I site at nt 2067, yielding the junction sequences of nt 1962 to 2069, 5′ TGT TTC **AAT TCC TGC AGC CCG GGG GAT CCG CGG GGT** ACT 3′, where the linker sequence is in boldface type and the HIV sequence is in normal type. Similarly, ΔNC deletes from the *Apo*I site at nt 1902 to the *Rsa*I site at nt 2067 (5′ ACA **AAT TCC TGC AGC CCG GGG GAT CCG CGG GGT** ACT 3′ [nt 1899 to 2069]), and Δp7bf deletes from nt 1932 to 2094 (5′ ATG CAG AGA GGC **GGG GAT CGA TCC CAT C**AG ATC TGG CCT 3′ [nt 1920 2105]). Of these deletions, ΔMun and ΔNC retain *pol* gene functions, but Δp7bf, which disrupts the *pol* frameshift signal, does not.

Three p6 mutations also were investigated. The p6 termination mutations p6T1 and p6T2 have linker insertions at the HIV-1 *Bgl*II site at nt 2096, resulting in the terminations of the *gag* ORF before the p6 coding region while the *gag-pol* ORF is not terminated. The junction region for p6T1 is nt 2094 to 2105, 5′ AAG ATC TGA TAT CAT CGA TGA ATT CGA GCT CGG TAC CCG GGG ATC TGG CCT 3′, while the junction region for p6T2 is nt 2094 to 2105, 5′ AAG ATC CCC GGG TAC CGA GCT CGA ATT CAT CGA TGA TAA CAG ATC TGG CCT 3′ (termination codons are underlined). The internal deletion Δp6 deletes nucleotides from the HIV-1 *Bgl*II site (nt 2096) to the compatible *Bcl*I site at 2429. With this mutation, the *pol* frame is retained; however, the protease-coding region in the *pol* frame is partially deleted such that the mutant is protease minus.

Cell culture. Cos7 cells were maintained in Dulbecco's modified Eagle's medium (DMEM) supplemented with 10% heat-inactivated fetal calf serum and penicillin plus streptomycin. For calcium phosphate transfections, 20- to 30%-confluent Cos7 cells on 10-cm-diameter plates were transfected as described previously (21, 66, 67, 68). Ordinarily, medium supernatants and cells were collected at 72 h posttransfection, but for time course experiments, at 48 h posttransfection, plates were mock treated or cycloheximide was added to each plate to a final concentration of 100 μg/ml. After a 15- to 20-min incubation, the medium was aspirated, cells were washed three times with 5 ml of DMEM plus fetal calf serum, and each plate was refed with 10 ml of medium ± 100 μg of cycloheximide per ml. At subsequent time points after refeeding, cells and medium supernatants were collected and processed for protein gels. For immunofluorescence experiments, confluent Cos7 cells from 10-cm-diameter plates were split 1:40 onto coverslips 24 h before being transfected with wt or mutant plasmids and transfected cells were processed for immunofluorescence 2 days later.

Gag protein analysis. At 72 h posttransfection, medium supernatants were collected and centrifuged at 4°C for 10 min at 1,000 × *g* to remove cell debris. For virus release assays, the cell-free supernatants were then centrifuged through 2 ml of 20% sucrose cushions in TSE (10 mM Tris hydrochloride, 100 mM NaCl, 1 mM EDTA, 0.1 mM phenylmethylsulfonyl fluoride [PMSF]) at 4°C for 45 min at 274,000 × *g* (SW41 rotor at 40,000 rpm; 2 ml of cushion for 10 ml of supernatants from each plate). The pellets were resuspended in 100 μl of IPB (20 mM Tris hydrochloride [pH 7.5], 150 mM NaCl, 1 mM EDTA, 0.1% sodium dodecyl sulfate [SDS], 0.5% sodium deoxycholate, 1% Triton X-100, 0.002% sodium azide) plus 0.1 mM PMSF. Cells were washed twice with 10 ml of ice-cold phosphate-buffered saline (PBS) and then collected into 2 ml of PBS in a 15-ml falcon tube for each 10-cm-diameter plate. Cells were then pelleted at 4°C for 10 min at 1,000 × *g*. The cell pellets were lysed in 1 ml of IPB plus 0.1 mM PMSF, followed by 10 min of microcentrifugation at 13,700 × *g* to remove debris. Cell lysate samples of 100 μl were aliquoted for virus release assays, while the rest was saved. Equal volumes of 2× sample buffer (12.5 mM Tris hydrochloride [pH 6.8], 2% SDS, 20% glycerol, 0.25% bromophenol blue) and 1/10 volume of β-mercaptoethanol were then added to the 100 μl of IPB suspensions of the virus and cell samples. After 5 min of boiling, samples were fractionated by SDS-polyacrylamide gel electrophoresis (PAGE) along with an internal control recombinant HIV CA standard for Gag protein quantitation purposes. After SDS-PAGE and electroblotting onto nitrocellulose filters, Gag proteins were immunodetected with mouse anti-HIV CA monoclonal antibody from hybridoma cell line Hy183 (made by Bruce Chesebro and obtained from the AIDS Research and Reference Reagent Program, Division of AIDS, National Institute of Allergy and Infectious Diseases [NIAID], National Institutes of Health [NIH]) as the primary antibody and an alkaline phosphatase-conjugated goat anti-mouse immunoglobulin G as the secondary antibody. HIV Gag proteins immunodetected on the nitrocellulose membranes were quantitated with DeskScan II, version 2.0 alias, and NIH image 1.59/fat software, and levels were normalized with the internal control recombinant HIV CA. For analysis of proteolytic processing, viral Gag precursor and intermediate- and final-processing product levels were calculated as percentages of the total amount of Gag present in a sample. For limiting antibody dilution experiments, virus pellets of the wt and 2498T were resuspended and aliquoted for protein gels. The virus samples were electroblotted in parallel onto a nitrocellulose membrane and detected with dilutions of the primary antibody.

For sucrose density gradient fractionations (23, 32, 66), 72 h posttransfection, supernatants were collected from three 10-cm-diameter plates of transfected Cos7 cells and centrifuged at 4°C for 10 min at 1,000 × *g* to remove cell debris. Cell-free supernatant material was pelleted by centrifugation (4°C, 2 h at 83,000 × *g*, SW28 rotor) through 4 ml of 20% sucrose cushions, resuspended in 200 μl of PBS, mixed with internal control Moloney murine leukemia virus (M-MuLV), and layered onto linear 20 to 60% sucrose gradients in TSE buffer in SW50.1 rotor polyallomer tubes. The gradients were centrifuged at 4°C for 24 h at 240,000 × *g* (equilibrium for particles of size 3S or greater). After centrifugation, 400-μl fractions were collected from the top to the bottom of the gradients. Each fraction was aliquoted for measurement of density and levels of HIV and M-MuLV Gag proteins.

To assay the subcellular localization of wt and mutant Gag proteins by immunofluorescence, 48 h after transfection of cells on coverslips, cells were fixed, permeabilized, and processed for indirect immunofluorescence by following standard methods (32, 66). The primary antibody was a tissue culture supernatant of hybridoma cell line Hy183 used undiluted, and the secondary antibody was rhodamine-conjugated anti-mouse immunoglobulin G antibody used at a 1:300 dilution. After the final washes with DMEM plus 10% heat-inactivated calf serum, penicillin, streptomycin, and 10 mM HEPES, pH 7.4, coverslips were washed three times for 5 min in PBS and mounted on slides in 50% glycerol in PBS. Cells were viewed and photographed with a Leitz Dialux 22/22 EB immunofluorescence microscope equipped with a standard rhodamine filter.

RNA analysis. For RNA isolation from cell-free-medium supernatants, particles were pelleted through 4 ml of 20% sucrose cushions at 4°C for 2 h at 83,000 × *g* (SW28 rotor). The virus pellets were resuspended in 600 μl of IPB, and a 100-μl aliquot was taken for protein analysis. To the rest of each of the suspensions (500 μl), 30 μg of carrier *Saccharomyces cerevisiae* tRNA was added, and samples were phenol-chloroform extracted twice, chloroform extracted twice, ethanol precipitated, and resuspended in 100 μl of TE buffer (10 mM Tris [pH 7.4], 1 mM EDTA). For cellular RNA preparation, cells from three transfection plates were washed twice with ice-cold PBS, collected into 2 ml of PBS, and pelleted at 4°C at 1,000 × *g* for 10 min. The cell pellets were lysed with 3 ml of GTC buffer (6 M guanidium thiocyanate, 25 mM sodium citrate [pH 7.0], 0.5% Sarkosyl, 100 mM β-mercaptoethanol), loaded on a 2-ml cushion of 6.2 M cesium chloride–100 mM EDTA (pH 7.0), and then centrifuged at 15°C for 18 h at 115,000 × *g* (SW 50.1 rotor). The pellets were washed with 70% ethanol, air dried, quantitated spectrophotometrically, and stored at −80°C.

An antisense probe for RNase protection assays was prepared from Blue HX 680-831 by in vitro transcription with T3 polymerase according to standard methods (67). The ^{32}P-labeled probe is 183 bases in length, including 5′ and 3′ non-HIV sequences derived from the pBluescribe (Stratagene) vector. HIV-1 spliced and unspliced genomic RNAs were expected to yield protected fragments of 64 and 150 bases, respectively. For riboprobe hybridizations, 10% of the viral RNA samples or 40 μg of the cellular RNAs was mixed with 10 μg of yeast tRNA, ethanol precipitated, dried, and resuspended for use. Hybridizations, RNase digestions, electrophoresis, and detection of protected RNA bands have been described previously (67). Protected bands on X-ray films and Gag protein signals from corresponding Western blots were processed by DeskScan II, version 2.0 alias, and NIH image 1.59/fat software for quantitation by following previously outlined methods (71).

RESULTS

Assembly of HIV-1 p2, NC, p1, and p6 mutants. Previous experiments have shown that the NC domain of HIV-1 is an important determinant for the efficiency of RNA packaging (1, 3, 11, 16, 19, 31, 42). In vitro and in vivo evidence also suggests that HIV-1 NC exerts some effect on the specificity of viral RNA encapsidation (6, 7, 12, 14, 33, 41, 57, 71). With regard to virus assembly, previous work has shown that the HIV-1 p2, NC, p1, and p6 regions influence particle assembly or release

(10, 38) and in some systems, RNA appears to have an impact on assembly or release processes (8). To further elucidate the function of the C-terminal region of HIV Gag, we decided to examine the effects of mutations in the p2, NC, p1, and p6 domains of HIV-1 on particle release and RNA encapsidation. The constructs used are illustrated in Fig. 1 and were based on a parental wt construct, HIVgpt, in which the HIV *env* gene was replaced by a *gpt* gene driven by the simian virus 40 origin of replication and early promoter (52, 66, 67); when the construct is transfected into Cos7 cells, Env-minus but otherwise wt virus particles can be produced from this construct. In addition to wt HIVgpt, we also have used a *pol* ORF truncation mutant, 2498T (Fig. 1), which produces nonprocessed immature virus particles (43). Within the p6 coding region, we created the premature Gag termination mutants p6T1 and p6T2, which retain PR function, and Δp6, which is PR deficient. Also available were *Bgl*II, a linker insertion mutation in p1, and two directed mutations in NC, namely, *Apa*I, a linker insertion between the Cys-His finger motifs, and A15, which possesses site-directed mutations of cysteines in the second zinc finger motif (1). Major NC mutations included internal deletions (ΔMun, Δp7bf, and ΔNC) and premature terminations (MunTE, TARK, TAM, and ApoTE). Of the internal deletion constructs, ΔMun removed the two Cys-His fingers but retained p2, p1, the amino- and carboxy-terminal segments of NC, and the *pol* frame. The Δp7bf and ΔNC mutations similarly deleted almost all of the NC domain, but Δp7bf excised part of p1 and was PR^- while ΔNC excised part of p2 and was PR^+. The truncation mutations also removed large portions of NC, and all of these were PR^-. They differ in the placement of translation terminations: for MunTE, the *gag* ORF terminates at the start of the first Cys-His motif, 17 codons into NC; for TARK, the *gag* ORF terminates 6 codons sooner; for TAM, translation stops exactly at the end of p2; and for ApoTE, translation terminates halfway through p2. The final mutation, ApoMTRB, was based on ApoTE but consisted of the replacement of the HIV-1 Gag NC, p1, and p6 domains with the *B. subtilis* RNA binding protein MtrB (49).

The abilities of the above-described mutant constructs to direct virus particle formation were studied in transiently transfected Cos7 cells. At 72 h after transfection of DNAs into Cos7 cells, medium supernatant and cell lysate samples were prepared, fractionated by SDS-PAGE, and electroblotted onto nitrocellulose membranes. The HIV Gag proteins then were immunodetected with an anti-HIV-CA antibody as detailed in Materials and Methods. A rough indication of the release efficiencies of wt and mutant constructs could be obtained by comparison of Gag protein levels in medium versus cell samples, and examples of immunoblot results are shown in Fig. 2. As illustrated in Fig. 2A, lanes A and B, wt HIVgpt Gag proteins appeared to release particles efficiently, as evidenced by the relatively high levels of Gag proteins present in the medium (lane A) versus the cell (lane B). Similarly, the PR^- but otherwise wt construct, 2498T, also directed the efficient release of Gag proteins from transfected cells (Fig. 2B, lanes A and B). Compared with HIVgpt or 2498T, it was apparent that certain mutants, notably ΔNC (Fig. 2A, lanes C and D), ApoTE (Fig. 2B, lanes C and D), and TAM (Fig. 2B, lanes G and H), released Gag proteins inefficiently.

In the process of quantitating Gag protein release values, a disparity was observed for the release of proteolytically processed versus unprocessed Gag proteins. In particular, when release levels of wt and 2498T were compared, it appeared that release from the PR^- construct (2498T) was more efficient than that of the wt (compare Fig. 2, lanes A and B). There are several potential reasons for the apparent difference in PR^- and PR^+ virus assembly and release. Released, unprocessed virus particles may be more stable than processed ones. Alternatively, the antibody used in detection might react better to the precursor Gag than the cleavage product CA, leading to an underestimation of the Gag proteins of the processed virus particles in the medium. Or, in transfected cells, if Gag proteins from the PR^- construct are less stable than Gag proteins from the wt construct, the construct may show an artificially high ratio of Gag protein levels outside versus inside cells. Finally, the Gag protein release rate for our transfection system might be higher for PR^- than for PR^+ constructs. We performed several experiments to distinguish between these possibilities (Fig. 3). The results shown in Fig. 3E showed that the extracellular stabilities of Gag proteins from PR^+ and PR^- constructs were similar, and antibody dilution experiments (Fig. 3F) suggested that our antibody reacts equally well to precursor, partially processed, and mature forms of Gag. These results implied that the observed differences in levels of release derived from differences in the cellular handling of the proteins. To examine cellular processes, medium supernatant and cell samples were collected at various time points from Cos7 cells transfected with wt (PR^+) and 2498T (PR^-) constructs (Fig. 3A and B). Although intracellular Gag protein levels remained roughly steady during the time course, the relative amount of virus release for the PR^- construct exceeded that for the PR^+ construct by 3- to 10-fold, suggesting more efficient release for the PR^- construct. As shown in Fig. 3C and D, experiments were performed similarly, except that transfected cells were treated with cycloheximide prior to and during time course collections to assess intracellular Gag protein stabilities. As shown, cycloheximide greatly reduced Gag release from both PR^+ and PR^- construct-transfected Cos7 cells, suggesting that active synthesis might be required for efficient particle assembly and release. However, results also showed that under cycloheximide treatment, Gag protein stabilities were approximately 165 min for the wt and 280 min for the PR^- construct. These results indicate that the observed apparent higher level of release for PR^- Gag is not due to a low intracellular PR^- Gag stability. Rather, wt virus particles seem to be released from the transfected cells less quickly and the nonreleased Gag proteins appear to be degraded more quickly. These observations will be discussed (see below) in the context of previous studies (5, 29, 34, 54).

The results shown in Fig. 3 indicated that PR^- virus particles were released more efficiently than wt virus particles in our system. Consequently, for evaluation of assembly efficiencies, it was necessary to compare PR^+ mutants with the wt and PR^- mutants with 2498T (PR^-). The results of such comparisons are shown in Fig. 4, in which the relative levels of assembly efficiency of the PR^+ and PR^- constructs are shown. With the exception of the p6T1 and p6T2 constructs, all mutants appeared to assemble less efficiently than their wt counterparts. We believe the release levels for p6T1 and p6T2 appear anomalously high because they are processed less well than wt HIVgpt (see below). Insofar as other mutants were concerned, there was considerable variation in levels of Gag protein release. Some mutations, such as the linker insertions (*Apa*I and *Bgl*II), the site-directed Cys-His motif mutation (A15), and the PR^- p6 deletion (Δp6), reduced the efficiency of virus assembly about twofold or less. However, major deletions and truncations of the NC region significantly reduced the levels of assembly. Furthermore, it appeared that p2 and the amino terminus of NC were important to Gag protein assembly and release, as evidenced by the extremely low release ratios of ΔNC, ApoTE, and TAM constructs, in which deletions extended to the N terminus of NC or into p2. However, it is not

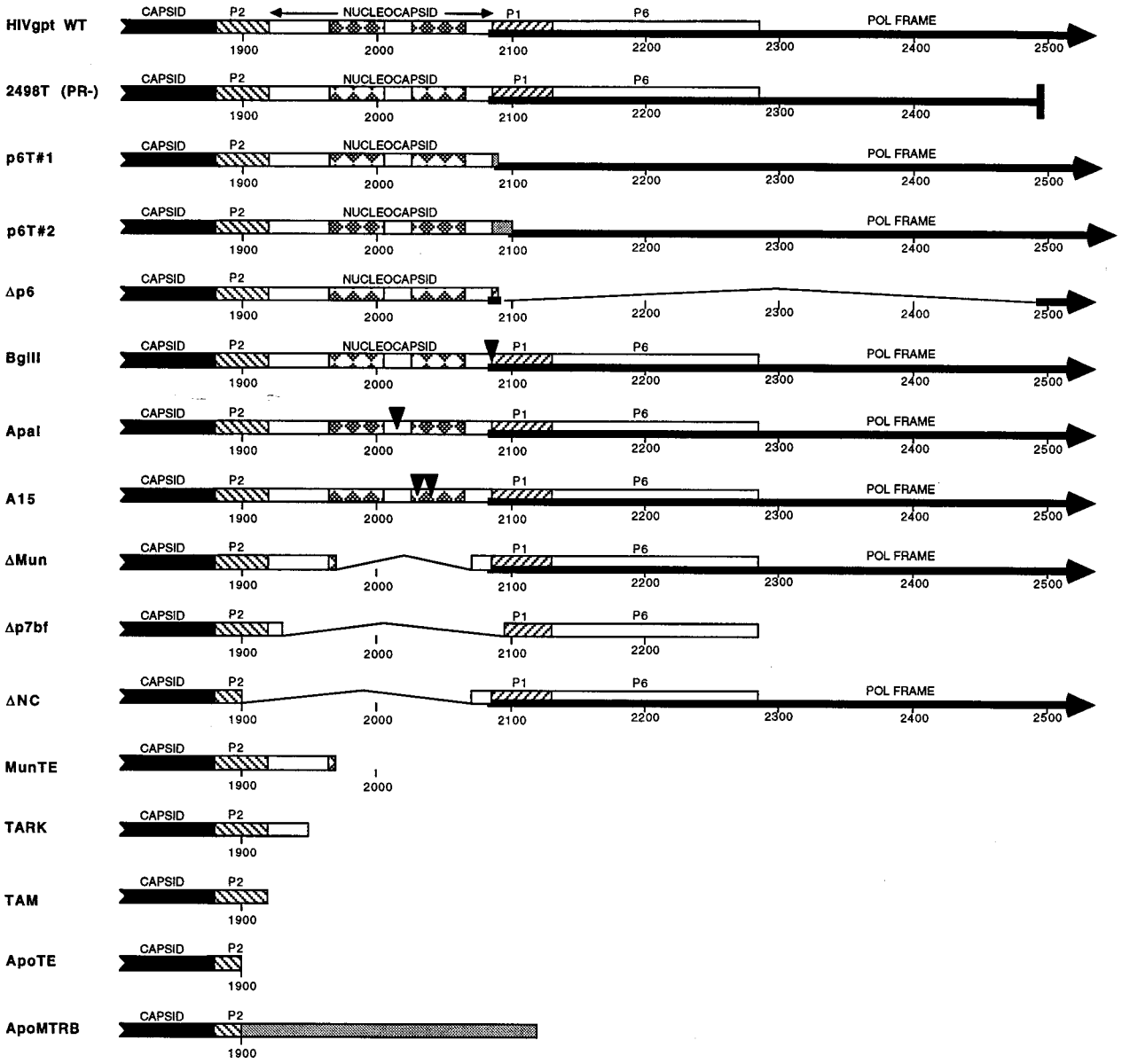

FIG. 1. Mutant HIV Gag constructs. The parental construct HIVgpt (55, 66, 67) is based on HIV HXB2 (17) and is diagrammed to show the C-terminal portion of the *gag* gene and the beginning of the *pol* gene. Only the C termini of CA, p2, NC, p1, and p6 of the *gag* ORF are shown in the diagram; they are labeled above their respective segments of the diagram. Cys-His motifs in the NC region are indicated as diamonds, and HIV-1 proviral nucleotide numbers are designated. An arrow indicates when the *pol* frame is intact. The construct 2498T has a terminator oligonucleotide insertion at the *Hin*dII site at nt 2498, stopping all three ORFs; it expresses wt Gag but not *pol* gene products (43). The p6 terminator mutations (p6T-1 and p6T-2) have linker insertions at the *Bgl*II site at nt 2096, resulting in the termination of Gag ORFs before the p6 coding sequences, while the *gag-pol* ORF is not terminated. In Δp6, the deleted HIV sequence from the *Bgl*II site at nt 2096 to the *Bcl*I site at nt 2429 is indicated by the thin lines in the diagram; the *gag-pol* frame is retained, although the PR coding region is disrupted, so the mutant is PR^{-}. *Bgl*II is a linker insertion mutant with a linker coding for 4 amino acid residues inserted at the *Bgl*II site at nt 2096 in p1, between the NC and p6 domains. *Apa*I is a mutant with a linker inserted at the *Apa*I site at nt 2010, which adds six codons between the two Cys-His motifs of the NC domain (66). In A15, the first two cysteine residues of the C-terminal NC Cys-His motif were mutated to tyrosine (1). Of the NC deletions, ΔMun and ΔNC retained the *pol* frame while Δp7bf was *pol* minus. Specific deletions were as follows: ΔMun (from the *Mun*I site [nt 1968] to the *Rsa*I site [nt 2067] removed the two zinc fingers of NC; ΔNC deleted the region from the *Apo*I site (nt 1900) in p2 to the *Rsa*I site at nt 2067; and Δp7bf deleted nt 1928 to 2096, leaving only four amino-terminal and four carboxy-terminal codons of the nucleocapsid domain. The terminator mutants MunTE, TARK, TAM, and ApoTE have oligonucleotide insertions which cause the Gag ORF to stop at different positions in p2 or NC, and neither p6 of the *gag* gene nor the *pol* gene is expressed. MunTE has an oligonucleotide at the *Mun*I site (nt 1968) and terminates translation 17 codons after the beginning of NC, before the two zinc fingers. TARK has an oligonucleotide inserted at the *Apo*I site at nt 1900 and should terminate translation 11 residues into NC. TAM and ApoTE also have sequences inserted at nt 1900, and TAM terminates precisely at the end of p2, while ApoTE causes the *gag* ORF to end in p2, five codons before the beginning of NC. Instead of terminating the *gag* ORF at the *Apo*I site at nt 1900 as in ApoTE, in ApoMTRB, the NC and p6 domains of HIV are swapped for a bacterial RNA binding protein, MtrB (49), which is indicated by a shaded bar. MtrB (8 kDa) is encoded by the methyltryptophan resistance (*mtr*) locus of *B. subtilis*, which is a two-gene operon consisting of *mtrA* and *mtrB*. MtrB has been shown to bind specifically to *trp* leader RNA in a tryptophan-dependent manner. Constructs with active *pol* frames have them indicated by arrows, and the precise sequences of the junctions of these constructs are provided in Materials and Methods.

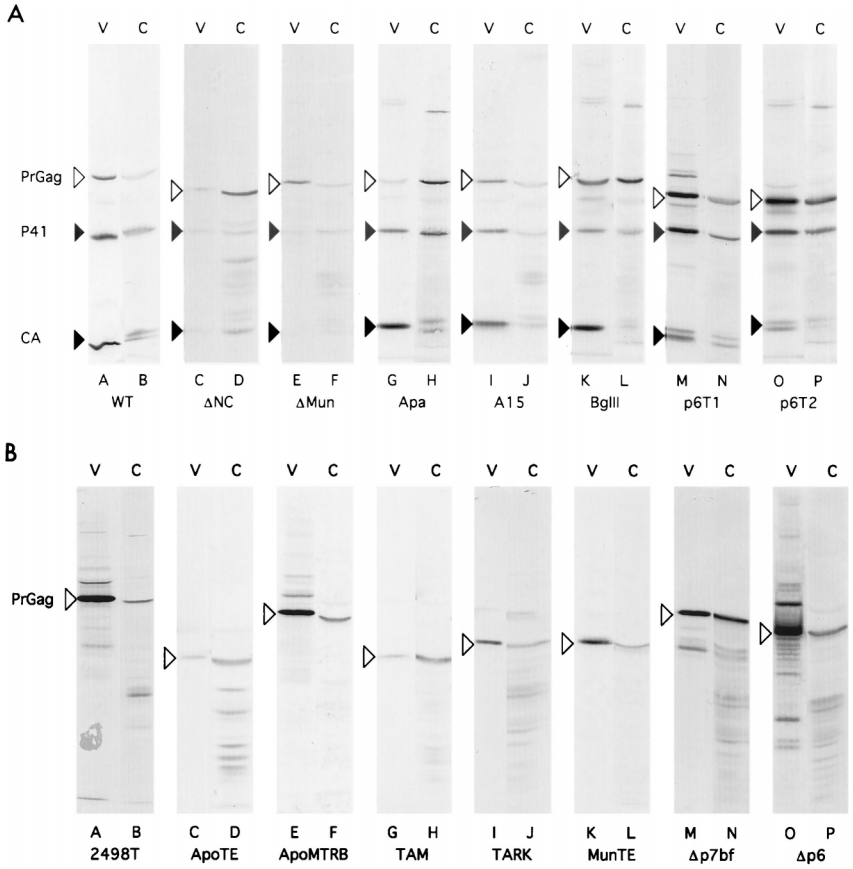

FIG. 2. Gag protein levels in cell lysate and medium samples. Medium supernatant (V) and cell (C) samples were collected 72 h after transfection of Cos7 cells with the indicated constructs. Particles were pelleted from medium samples and resuspended; half of each pelleted medium preparation was used for loading on SDS-polyacrylamide gels. Cell pellets were lysed and centrifuged to remove debris, and 1/20 of each cell lysate sample was prepared for SDS-PAGE. Gag proteins in samples were separated by SDS-PAGE, electroblotted onto nitrocellulose filters, and immunodetected with a mouse anti-p24 monoclonal antibody from hybridoma cell line Hy183 as the primary antibody. Precursor (open triangles), partially processed (shaded triangles), and mature (filled triangles) Gag proteins were identified by antibody reactivity and comparison of gel migration mobilities to known standards. For each of the two panels, medium samples are in lanes A, C, E, G, I, K, M, and O and cell samples are in lanes B, D, F, H, J, L, N, and P. (A) PR^+ constructs are the wt, ΔNC, ΔMun, *Apa*I, A15, *Bgl*II, p6T1, and p6T2. (B) PR^- constructs are 2498T, ApoTE, ApoMTRB, TAM, TARK, MunTE, Δp7bf, and Δp6.

clear how p2 and NC impact particle assembly: their contributions to this process may or may not be sequence specific. An argument against a sequence-specific requirement is that ApoMTRB, in which p2, NC, p1, and p6 are replaced by an unrelated sequence, directed the efficient release of chimeric Gag proteins.

As illustrated above (Fig. 2 and 4), some of our mutant proteins were not assembled and released efficiently, even though Gag proteins were readily detected within cells. It is possible that these mutant Gag proteins were blocked during transport to the cell surface, as has been observed previously for some mutant Gag proteins (23, 32, 66, 68). Alternatively, plasma membrane-localized proteins might have been defective in the processes of assembly or release. To find where Gag proteins resided in cells, we examined the subcellular localizations of wt and release-impaired truncation mutant Gag proteins (ApoTE, TAM, TARK, and MunTE) by immunofluorescence light microscopy. Our results indicated that wt Gag proteins stained as a perinuclear ring plus a heterogeneous pattern through the cell periphery, while ApoTE, TAM, TARK, and MunTE proteins showed heterogeneous nonnuclear staining, with staining along cell edges (data not shown). These results did not support the notion that ApoTE, TAM, TARK, and MunTE proteins were trapped at intracellular membranes but suggested that they were delivered to the cell surface, as has been reported for other NC mutant retroviruses (38).

Characterization of wt and mutant virus particles. In our virus assembly and release assays, collection of cell-free medium supernatant samples involved pelleting through 2 ml of 20% sucrose cushions for 45 min at 274,000 × *g*. Based on centrifugation clearing rates, the minimum particle size to pellet is 165S, and over 90% of our medium HIVgpt Gag protein was recoverable by this method in control experiments (data not shown).

These data suggest that wt and mutant Gag proteins were released from cells in particle forms. Although a complete analysis of each mutant virus awaits electron microscope analysis, biochemical characterization of the particles was also of interest. For Gag proteins produced from PR^+ constructs, one avenue of analysis was to examine whether released Gag proteins were processed by the viral protease. Consequently, CA, p41, and Pr^{Gag} levels in pelleted medium supernatant samples for PR^+ constructs were determined (Table 1). Not surprisingly the site-directed and linker insertion mutants (A15, *Apa*I, and *Bgl*II) were processed at approximately wt levels. The p6T1 and p6T2 proteins also were processed, albeit at lower efficiency than the wt. More dramatic were results for the

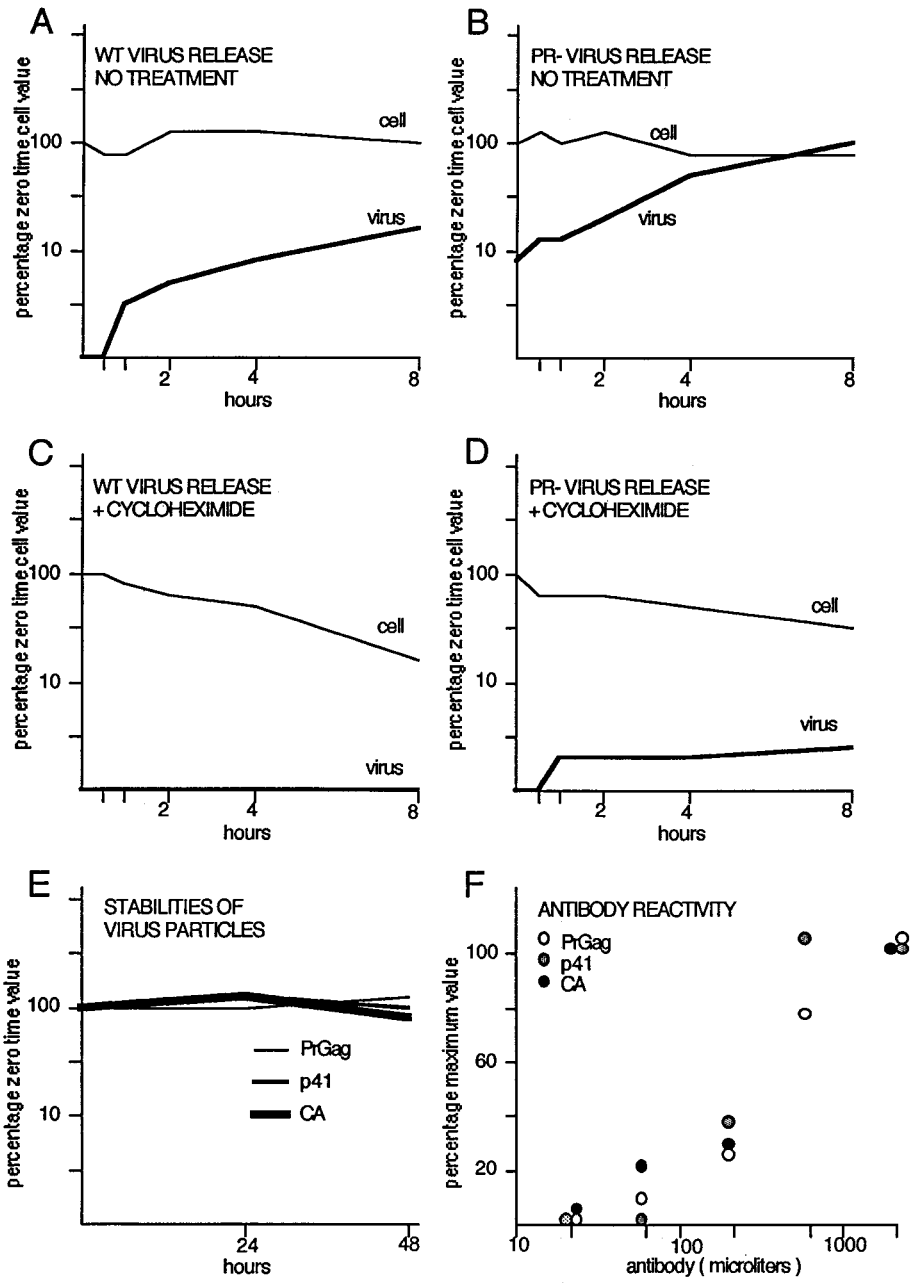

FIG. 3. Stability and release of Gag proteins. (A and B) At 48 h after transfection of Cos7 cells with wt HIVgpt (A) or 2498T (B), cells were washed and refed. At time points thereafter, cell (thin line) and medium supernatant (thick line) samples were collected and processed for immunodetection. Gag protein signals were quantitated for each time point and are plotted as percentages of the zero time cellular Gag value versus collection time. (C and D) Experiments were performed and results were plotted as in panels A and B, except that 100 μg (final concentration) of cycloheximide per ml was present in the wash, during a 20-min preincubation step, and throughout each time course. (E) Medium supernatants from wt- and 2498T-transfected Cos7 cells were collected and incubated 0, 24, or 48 h at 37°C, after which virus particles were pelleted and processed for immunodetection of Gag proteins. Results are plotted as percentages of zero time Gag protein levels versus collection times and are given for Pr^{Gag} proteins from 2498T particles and p41 and CA proteins from wt particles. (F) Equal aliquots of wt and 2498T particles were electrophoresed, electroblotted, and immunodetected in parallel with various dilutions of the mouse Hy183 anti-Ca monoclonal antibody. Gag protein signals were quantitated and are plotted as percentages of the maximum values of Pr^{Gag}, p41, or CA versus antibody dilutions. The p41 and CA results derive from wt particles, while Pr^{Gag} results derive from 2498T particles.

mutants which had major deletions in NC (ΔNC and ΔMun). Seventy percent or more of the Gag proteins synthesized by these two constructs remained unprocessed, suggesting that mutant Gag-Pol proteins do not assemble into virions or are impaired for PR activity or that Gag proteins are packed in such a way that they are not accessible for processing.

Another method for analysis of released particles is by density gradient fractionation. Retrovirus particles have densities of 1.140 to 1.180 g/ml, and while evidence has suggested that retroviral densities are not grossly dependent on RNA encapsidation levels, aberrant densities might be an indication of different arrangements of packing the Gag proteins within

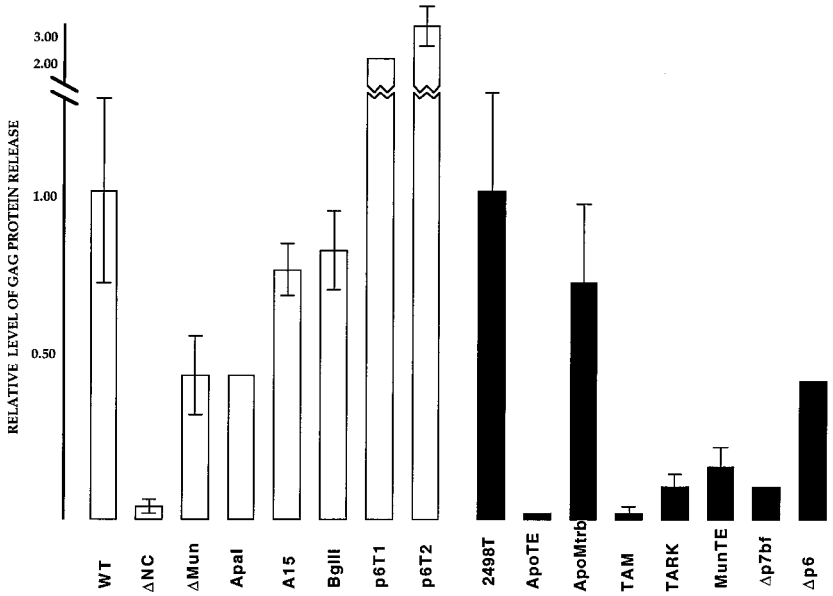

FIG. 4. Levels of Gag protein release from transfected cells. Gag proteins in matched cell and medium supernatant samples were detected as described in the legend to Fig. 2 and quantitated with the programs DeskScan II (version 2.0 alias) and NIH image 1.59/fat. After normalization of Gag protein levels with a bacterially expressed HIV CA protein standard run on each gel, ratios of the total Gag protein levels in the media versus in cells were calculated. The ratios of the PR^+ constructs (open bars) were normalized to that of wt HIVgpt, and the ratios of the PR^- constructs (filled bars) were normalized to that of 2498T. Thus, the higher the release ratio, the greater the level of Gag protein release. Note that the release ratio of 2498T was 2.6 times that of HIVgpt and that standard deviations are shown, when available.

virus particles (5). To measure the densities of wt and mutant particles, virus resuspensions recovered from the transfected Cos7 media were mixed with an internal control mouse retrovirus stock (Sup1 M-MuLV [56]) and fractionated by sucrose density gradient centrifugation. Collected fractions were assayed for density and Gag protein content (HIV and M-MuLV), and results are shown in Fig. 5. The fractionation profiles of the PR^+ constructs are shown in the left two columns for comparison with wt HIVgpt, while the profiles of PR^- constructs are shown in the right two columns for comparison with 2498T, since we found that processed wt HIVgpt particles came to equilibrium at a density of 1.148 g/ml (equal to that of M-MuLV) while the PR^- 2498T particles came to a density equilibrium of 1.168 g/ml (greater than that of M-MuLV). Relative to that of wt HIVgpt, the p6 terminators (p6T1 and p6T2) showed higher densities, but since the p6T1 and p6T2 proteins were incompletely processed (Table 1), it was not surprising that they had densities similar to that of 2498T. *Apa*I, A15, *Bgl*II, TARK, MunTE, ΔMun, and Δp6 had densities similar to those of their wt counterparts, while ΔNC, ApoTE, TAM, and Δp7bf showed densities lower than those of their wt counterparts. These results suggest that p2 and the amino-terminal portion of NC are necessary for packing Gag proteins into wt-like virus: critical residues apparently map between the fourth (Δp7bf) and the eleventh (TARK) residues of NC, although the results with the ΔMun construct are not in strict agreement with this assessment. Interestingly, while ApoMTRB particles assemble and are released at reasonable levels of efficiency, the particles are of low density, at least compared with the PR^- 2498T particles. This result is reminiscent of some MuLV Gag fusion proteins (32) and suggests that high-density packing mediated by NC domains is not essential to efficient Gag protein release from cells.

TABLE 1. Proteolytic processing of HIV-1 Gag proteins

Construct	% of total viral Gag[a]		
	Pr^{Gag}	p41	CA
wt	20.8 ± 7.6	20.9 ± 8.6	58.3 ± 12.9
ΔNC	69.9 ± 17.8	15.9 ± 14.9	14.2 ± 15.8
ΔMun	92.2 ± 0.8	6.1 ± 1.1	1.7 ± 1.8
Apa	20.2 ± 10.6	23.6 ± 9.0	56.2 ± 14.6
A15	14.9 ± 7.4	31.4 ± 7.5	53.7 ± 11.1
*Bgl*II	37.8 ± 8.6	9.7 ± 3.7	52.5 ± 11.5
P6T1	33.5 ± 1.0	26.2 ± 1.2	40.3 ± 0.6
P6T2	47.2 ± 6.8	32.4 ± 6.2	20.4 ± 11.9

[a] Medium supernatant pellets from Cos7 cells transfected with the indicated constructs were fractionated by SDS-PAGE, electroblotted, and immunodetected as described in the legend to Fig. 2. The particle-associated Pr^{Gag}, partially processed p41, and CA protein signals were quantitated and are expressed in the table as percentages of the total Gag protein signals of the respective samples. Multiple experiments were carried out to obtain the averages and the standard deviations; the numbers of experiments averaged to obtain values were as follows: 30 for the wt, 5 for ΔNC, 2 for ΔMun, 8 for *Apa*I, 13 for A15, 3 for *Bgl*I, 3 for p6T1, and 6 for p6T2.

Encapsidation of retroviral RNA. Efficient and selective encapsidation of viral genomic RNA into virus particles requires incompletely defined interactions between virus core proteins and the viral encapsidation signal, which appears to be localized near the 5′ portion of the HIV-1 RNA (1, 11, 25, 40). To examine viral RNA packaging into wt and mutant particles, Cos7 cells were transiently transfected with wt or mutant constructs and cellular and viral RNAs were isolated 72 h post-transfection, as described in Materials and Methods. Aliquots also were taken from virus preparations prior to RNA isolation for Gag protein quantitation. A quantitative RNase protection assay (67, 71) was employed to measure the viral RNAs present in cells and particles, using an antisense riboprobe designed to span the major splice donor site, which allowed

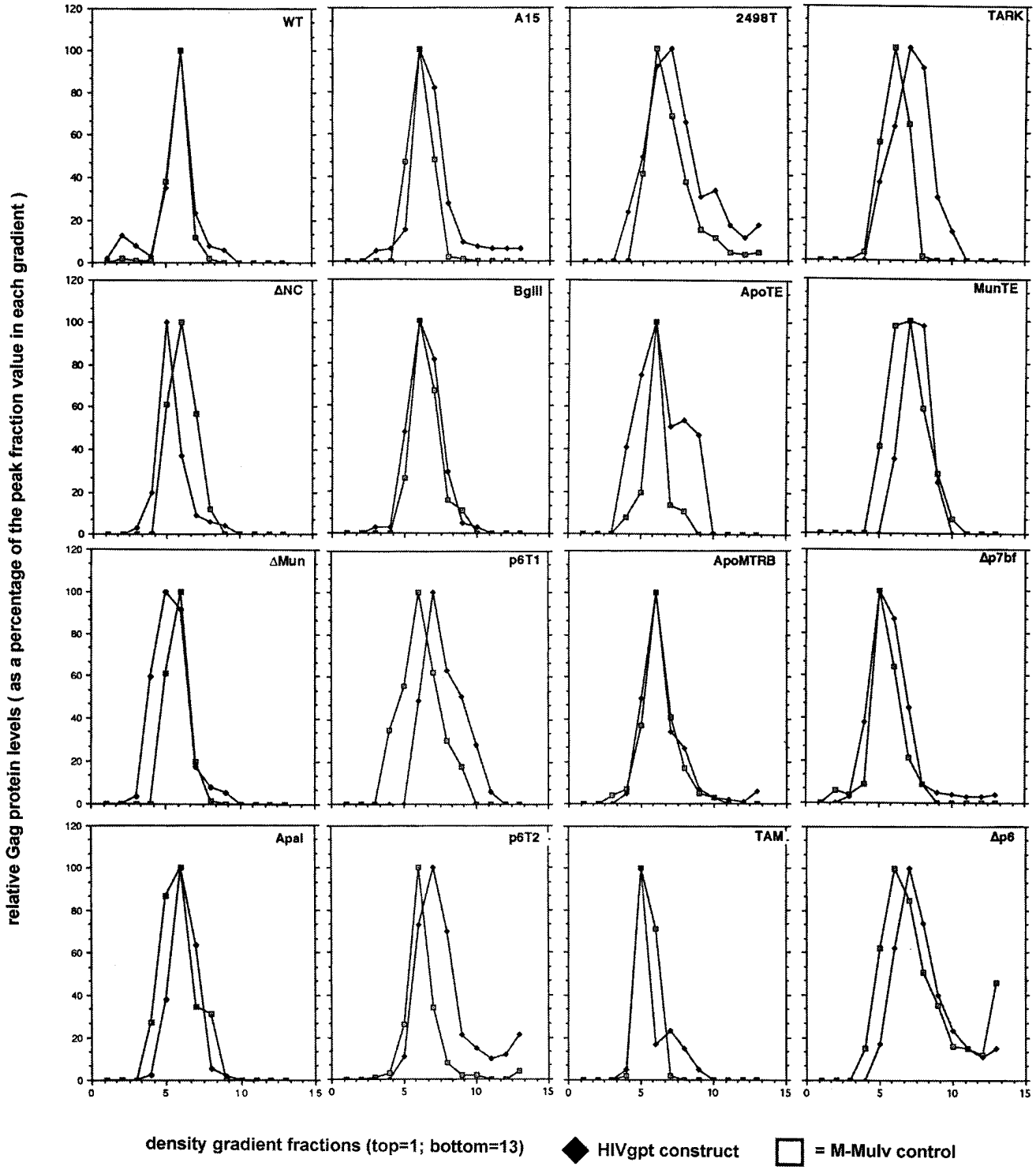

FIG. 5. Sucrose density gradient fractionation of wt and mutant HIV-1 particles. Virus pellets prepared from 30 ml of cell-free supernatants from transfected Cos7 cells were resuspended in 200 μl of PBS, mixed with mouse M-MuLV suspensions, and layered on top of the linear 20 to 60% sucrose gradients. Gradients were centrifuged for 24 h at 240,000 × *g* so that particles with a sedimentation coefficient of 3S or greater would come to equilibrium. After centrifugation, 400 μl-fractions were collected from the top to the bottom and each fraction was monitored for density and for HIV-1 and M-MuLV Gag protein content. Gag protein bands were quantitated with the DeskScan II (version 2.0 alias) and NIH image 1.59/fat programs, and HIV or M-MuLV Gag protein levels in fractions are expressed as percentages of the respective peak fraction values. The *x* axes indicate the density gradient fractions from top (left, low numbers) to bottom (right, high numbers). The peak densities of each gradient were 1.152 g/ml for the wt, 1.137 g/ml for ΔNC, 1.131 g/ml for ΔMun, 1.150 g/ml for *Apa*I, 1.148 g/ml for A15, 1.161 g/ml for *Bgl*II, 1.164 g/ml for p6T1, 1.177 g/ml for p6T2, 1.168 g/ml for 2498T, 1.155 g/ml for ApoTE, 1.155 g/ml for ApoMTRB, 1.140 g/ml for TAM, 1.180 g/ml for TARK, 1.160 g/ml for MunTE, 1.146 g/ml for Δp7bf, and 1.182 g/ml for Δp6.

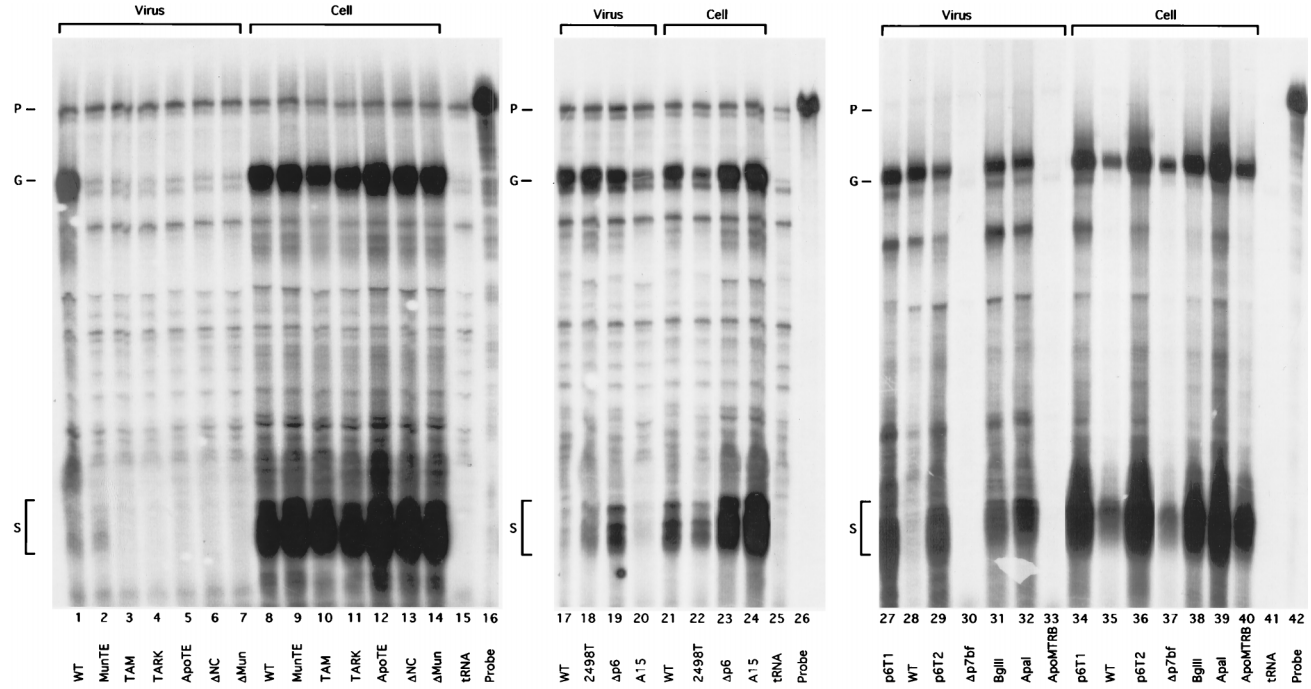

FIG. 6. Genomic and spliced RNA levels in cells and virus particles. RNA samples were prepared from transfected cells and virus pellets, as described in Materials and Methods. RNAs (10% of viral samples or 40 μg of the cellular samples) were mixed with 10 μg of yeast tRNA, ethanol precipitated, dried, and processed for RNase protection assays with an antisense probe (P) of 183 nt (lanes 16, 26, and 42) capable of detecting both spliced viral transcripts (S) at a fragment size of 63 to 64 nt and unspliced genomic RNAs (G) at a protected fragment size of 150 nt. In each panel, results from mock reactions with yeast tRNA samples were also used (lanes 15, 25, and 41). Lane contents (experimental virus [listed first] and cell [listed second] samples) are as labeled on the figure. Note that viral RNA signals were normalized for total Gag protein content to yield encapsidation efficiencies as described in Materials and Methods.

differentiation of full-length viral genomic RNA and spliced viral transcripts. Examples of the protection gels are shown in Fig. 6. The probe of 183 bases long is shown in lanes 16, 26, and 42, and little background protection was detected with the control yeast tRNA samples (lanes 15, 25, and 41). As expected, wt HIVgpt was expressed well in the transfected Cos7 cells (lanes 8, 21, and 35), showing bands corresponding to viral full-length (150-nt) and spliced (64-nt) RNAs. Full-length viral RNA was detected in particles released from wt HIVgpt-transfected cells, but little spliced viral RNA could be detected in the particles (lanes 1, 17, and 28), indicating that full-length genomic RNA was efficiently and specifically packaged into wt virus particles. Similar results were obtained with the PR^- construct, 2498T (lanes 18 and 22). By comparison, all mutants showed high levels of full-length genomic and spliced RNAs in cellular RNA samples (lanes 8 to 14, 21 to 24, and 34 to 40). However, the constructs with major NC deletions, truncations, or replacements showed no RNA in the particle samples (lanes 2 to 7, 30, and 33). As seen previously (71), A15, in which cysteines of the second Cys-His motif of NC were mutated to tyrosines, showed a reduced level of HIV RNA in the virus particles and a lower ratio of genomic versus spliced RNA, suggesting that the zinc finger affects both packaging efficiency and specificity. The other constructs, *Apa*I (lanes 32 and 39), *Bgl*II (lanes 31 and 38), and the three p6 mutants (lanes 19 and 23, 27 and 34, and 29 and 36) all appeared to show efficient genomic RNA encapsidation, but reduced specificity, as evidenced by high levels of spliced RNA in virus particles.

To evaluate encapsidation results, cell and virus protection band signals and their corresponding Gag protein signals from Western blots were quantitated with DeskScan II, version 2.0 alias, and NIH image 1.59/fat software programs. From these data, ratios were calculated for virus RNA versus cell RNA, virus RNA versus virus Gag protein, and virus genomic RNA versus virus spliced RNA. Values, normalized to wt HIVgpt results, are given in Table 2. As shown, the PR^- 2498T construct gave no clear-cut indication of a loss of encapsidation efficiency but appeared to show a somewhat increased tendency to package spliced transcripts. However, less subtle results were obtained for other mutants. Notably, all deletions or truncations that removed the HIV-1 NC Cys-His fingers failed to package viral RNA. This result also applied to ApoMTRB, in which the NC, p1, and p6 domains are replaced with the unrelated *trp* leader RNA binding protein encoded by the *B. subtilis* methyltryptophan resistance (*mtrB*) gene. Results for A15, the construct with the site-directed Cys-His finger mutation, showed reduced packaging efficiency and specificity, as observed previously (71). The situation was slightly different for the linker insertion between the two NC fingers (*Apa*I), the insertion in p1 (*Bgl*II), and the p6 deletions and truncations. All of these appeared to package RNA efficiently, with virus-to-cell RNA ratios of at least 80% of wt levels, and particle-RNA-to-Gag ratios at least half that of the wt. However, the encapsidation specificities for these mutants were clearly reduced, as indicated by particle-associated unspliced-to-spliced-RNA ratios 8 to 25% of that of the wt. These results indicate that both the NC and p6 domains contribute to the specificity of HIV RNA encapsidation, although p6 may act indirectly, by influencing NC folding.

DISCUSSION

It has been shown that mutations affecting retrovirus NC Cys-His motifs can reduce levels of genomic RNAs packaged

TABLE 2. RNA encapsidation into virus particles[a]

Construct	Total viral RNA in a virus sample vs that in a cell sample	Total viral RNA/viral gag protein	Viral genomic RNA/viral spliced RNA
wt	100.0	100.0	100.0
2498T (PR^-)	328.6	67.4	51.8
*Apa*I	84.4	55.7	17.3
A15	14.3	31.7	39.1
*Bgl*II	84.4	52.9	25.0
P6T1	118.8	52.1	12.8
P6T2	106.3	62.1	8.7
Δp6	89.8	51.6	19.8
ΔNC	<1.0	<1.0	NA
ΔMun	<1.0	<2.0	NA
ApoTE	<1.0	<1.0	NA
ApoMTRB	<1.0	<1.0	NA
TAM	<1.0	<1.0	NA
TARK	<1.0	<1.0	NA
MunTE	<9.5	<8.0	NA
Δp7bf	<1.0	<1.0	NA

[a] Genomic and spliced RNA signals from cell and virus samples listed in Fig. 6 and corresponding Gag protein levels from virus particles detected by Western blots were quantitated with DeskScan II (version 2.0 alias) and NIH image 1.59/fat software. From these data, the following ratios were calculated for each indicated construct; the total level of viral spliced and unspliced RNAs in a particle sample divided by that of a cell sample, the total particle-associated viral RNA signal divided by the particle Gag protein signal, and the particle genomic RNA signal divided by the particle spliced viral RNA signal. Calculated ratios were normalized to wt HIVgpt ratios and are listed as percentages of wt levels (wt = 100%). For mutants which showed no particle-associated viral RNA signal above background, values in the second and third columns are given as less than a given level, while values for the right-most column were not applicable (NA). Note that although some mutants released particles very inefficiently, experiments were scaled up as necessary to obtain the Gag-normalized levels in the third column of the table.

into retrovirus particles (1, 3, 11, 16, 19, 31, 45), although the extent to which NC contributes to encapsidation specificity has not been elucidated completely (6, 7, 12, 33, 41, 57, 71). In addition to its function in RNA encapsidation, NC and the C-terminal portions of retroviral Gag proteins appear to possess a region involved in increasing the efficiency of virus particle assembly; this region has been referred to as an assembly domain (5), although its exact contribution to virus assembly is not clear (10, 15, 18, 20, 27, 38). Our study focused on the evaluation of the effects of the p2, NC, p1, and p6 domains of HIV-1 on virus assembly and RNA encapsidation.

In accord with previous observations (33, 37), major deletions, truncations, or replacements of the NC domain of HIV-1 *gag* were found to eliminate the encapsidation of HIV genomic or spliced RNAs into virus particles. Although they are theoretically possible, we do not believe these results are due to a defect of mutant construct *cis*-active encapsidation (Psi) signals, since the mutations occurred away from the known Psi signals (4, 24, 25, 42, 57). We have not measured the content of nonviral RNAs in these mutant particles, but if packaging of spliced viral RNA is an indication of nonspecific RNA encapsidation, we would expect little RNA of any kind in these virus particles, although this assumption has yet to be proven. While major NC mutations apparently eliminated encapsidation, other mutants showed more subtle effects. Linker insertion between the two NC zinc fingers in the mutant *Apa*I reduced the specificity of encapsidation, while the total amount of RNA packaged was normal. This observation supports the previously described model that NC contributes to the specificity of RNA encapsidation (7, 71). Perhaps more surprisingly, mutants of p1 or p6 maintained wt levels of encapsidated RNA, but their specificities of RNA encapsidation were reduced (Fig. 6; Table 2). This strongly suggests that Pr^{Gag} determines packaging specificity and implicates the entire C-terminal region of HIV-1 Gag in the process.

The PR^- construct, 2498T, seemed to release particles more efficiently than wt HIVgpt in our experimental system. This result differs somewhat from results with avian (63) and murine (13, 36) retroviruses in which protease activity does not appear to affect release levels and contrasts with results of one study of HIV, in which PR^- particles were released less efficiently than PR^+ particles (34). It is unclear how the PR^+ phenotype might impair transport of Gag protein or establishment of interprotein contacts required for assembly and budding, although a number of studies have shown that perturbation of Gag protein-to-PR activity ratios can alter virus release efficiencies (29, 34, 44, 53, 54). Because of the differences observed with wt HIVgpt and 2498T, we compared mutant particle release efficiencies with that of either wt HIVgpt or 2498T, depending on the PR phenotype of the mutant construct (Fig. 4). In performing such comparisons, we observed that mutants without p6 were released at reasonable efficiencies, which is consistent with the notion that the effects of p6 on virus release may be affected by PR or may be cell type specific (29, 34, 44, 61). However, constructs with mutations in p2 and the amino-terminal portion of NC were released much less well than the wt, supporting the notion that this region defines an assembly domain which appears to function after Gag protein delivery to the plasma membrane (Fig. 3) (10, 38, 69, 70). Still, it is not evident how this region contributes to the efficiency of HIV-1 assembly, since replacement of this region with the unrelated sequence in ApoMTRB permitted efficient release of virus-like particles. This result is reminiscent of the ability of some M-MuLV Gag fusion proteins to direct particle assembly (23, 32), and the ability of ApoMTRB proteins to release particles at reasonable efficiency might be interpreted in several ways. One possibility is that the Mtrb domain may prevent the C terminus of CA from folding into an assembly-incompatible conformation. Alternatively, the Mtrb domain may substitute for an active assembly function of p2 or NC. One might favor the first of these alternatives, since in addition to the assembly and release of HIV Gag-Mtrb particles, we have observed that MuLV Gag fusions to β-galactosidase also form virus-like particles. However, both Mtrb and β-galactosidase proteins form higher-order oligomers (2, 30), so it may be that the essential assembly function provided by NC is a nonspecific ability to make interprotein contacts. Although the Mtrb domain was fused to HIV-1 *gag* because it potentially acts as an RNA binding protein (49), no evidence of specific or nonspecific RNA incorporation into ApoMTRB particles was observed in our experiments with either HIV RNA (Fig. 6) or Mtrb target RNA (data not shown). Thus, it appears that the NC assembly function can be replaced by that of a protein that does not encapsidate detectable levels of RNA in our system. We believe that further analysis of the mechanism(s) by which the NC assembly domain acts will be of basic and practical interest.

ACKNOWLEDGMENTS

We thank Marylene Mougel, Jason McDermott, Sonya Karanjia, Zachary Love, Chin-tien Wang, and Mark Hansen for help and advice throughout the course of this work. The anti–M-MuLV–CA monoclonal antibody was a gift from Bruce Chesebro, who also made the anti-HIV-CA Hy183 hybridoma cell line that was obtained from the AIDS Research and Reference Reagent Program, Division of AIDS, NIAID, NIH. A molecular clone encoding the Mtrb protein was kindly provided by Paul Gollnick, and the A15 clone originally was from Anna Aldovini.

This work was supported by grant 2RO1CA47088-07 from the National Cancer Institute.

REFERENCES

1. **Aldovini, A., and R. A. Young.** 1990. Mutations of RNA and protein sequences involved in human immunodeficiency virus type 1 packaging result in production of noninfectious virus. J. Virol. **64:**1920–1926.
2. **Antson, A. A., J. Otridge, A. M. Brzozowski, E. J. Dodson, G. G. Dodson, K. S. Wilson, T. M. Smith, M. Yang, T. Kurecki, and P. Gollnick.** 1995. The structure of trp RNA-binding attenuation protein. Nature **374:**693–700.
3. **Aronoff, R., A. M. Hajjar, and M. L. Linial.** 1993. Avian retroviral RNA encapsidation: reexamination of functional 5′ RNA sequences and the role of nucleocapsid Cys-His motifs. J. Virol. **67:**178–188.
4. **Baudin, F., R. Marquet, C. Isel, J.-L. Darlix, B. Ehresmann, and C. Ehresmann.** 1993. Functional sites in the 5′ region of human immunodeficiency virus type 1 RNA form defined structural domains. J. Mol. Biol. **229:**382–397.
5. **Bennett, R. P., T. D. Nelle, and J. W. Wills.** 1993. Functional chimeras of the Rous sarcoma virus and human immunodeficiency virus Gag proteins. J. Virol. **67:**6487–6498.
6. **Berkowitz, R. D., J. Luban, and S. P. Goff.** 1993. Specific binding of human immunodeficiency virus type 1 gag polyprotein and nucleocapsid to viral RNAs detected by RNA mobility shift assays. J. Virol. **67:**7190–7200.
7. **Berkowitz, R. D., A. Ohagen, S. Hoglung, and S. P. Goff.** 1995. Retroviral nucleocapsid domains mediate the specific recognition of genomic viral RNAs by chimeric Gag polyproteins during RNA packaging in vivo. J. Virol. **69:**6445–6456.
8. **Campbell, S., and V. Vogt.** 1995. Self-assembly in vitro of purified CA-NC proteins from Rous sarcoma virus and human immunodeficiency virus type 1. J. Virol. **69:**6487–6497.
9. **Cann, A. J., and J. Karn.** 1989. Molecular biology of HIV-1: new insights into the virus life cycle. AIDS **3**(Suppl. 1)**:**S19–S34.
10. **Carriere, C., B. Gay, N. Chazal, N. Morin, and P. Boulanger.** 1995. Sequence requirements for encapsidation of deletion mutants and chimeras of human immunodeficiency virus type 1 Gag precursor into retrovirus-like particles. J. Virol. **69:**2366–2377.
11. **Clavel, F., and J. M. Orenstein.** 1990. A mutant of human immunodeficiency virus with reduced RNA packaging and abnormal particle morphology. J. Virol. **64:**5230–5234.
12. **Clever, J., C. Sassetti, and T. G. Parslow.** 1995. RNA secondary structure and binding sites for *gag* gene products in the 5′ packaging signal of human immunodeficiency virus type 1. J. Virol. **69:**2101–2109.
13. **Crawford, S., and S. Goff.** 1985. A deletion mutation in the 5′ part of the *pol* gene of Moloney murine leukemia virus blocks proteolytic processing of the *gag* and *pol* polyproteins. J. Virol. **53:**899–907.
14. **Dannull, J., A. Surovoy, G. Jung, and K. Moelling.** 1994. Specific binding of HIV-1 nucleocapsid protein to PSI RNA in vitro requires N-terminal zinc finger and flanking basic amino acid residues. EMBO J. **13:**1525–1533.
15. **Dorfman, T., J. Luban, S. P. Goff, W. A. Haseltine, and H. G. Gottlinger.** 1993. Mapping of functionally important residues of a cysteine-histidine box in the human immunodeficiency virus type 1 nucleocapsid protein. J. Virol. **67:**6159–6169.
16. **Dupraz, P., S. Oertle, C. Meric, P. Danay, and P.-F. Spahr.** 1990. Point mutations in the proximal Cys-His box of Rous sarcoma virus nucleocapsid protein. J. Virol. **64:**4978–4987.
17. **Fisher, A. G., M. B. Feinberg, S. R. Josephs, M. E. Harper, L. M. Marselle, G. Reyes, F. A. Gonda, A. Aldovini, C. Debouk, R. C. Gallo, and F. Wong-Staal.** 1986. The transactivator gene of HTLV-III is essential for virus replication. Nature **320:**367–371.
18. **Gheysen, D., E. Jacobs, F. de Foresta, D. Thiriart, M. Francotte, D. Thines, and M. De Wilde.** 1989. Assembly and release of HIV-1 precursor $pr55^{gag}$ virus-like particles from recombinant baculovirus-infected cells. Cell **59:**103–112.
19. **Gorelick, R. J., S. M. Nigida, Jr., J. R. Bess, Jr., L. O. Arthur, L. E. Henderson, and A. Rein.** 1990. Noninfectious human immunodeficiency virus type 1 mutants deficient in genomic RNA. J. Virol. **64:**3207–3211.
20. **Gottlinger, H. G., J. G. Sodroski, and W. A. Haseltine.** 1989. Role of capsid precursor processing and myristylation in morphogenesis and infectivity of human immunodeficiency virus type 1. Proc. Natl. Acad. Sci. USA **86:**5781–5785.
21. **Graham, R., and A. van der Eb.** 1973. A new technique for the assay of infectivity of human adenovirus 5 DNA. Virology **52:**456–467.
22. **Haffar, O., J. Garrigues, B. Travis, P. Moran, J. Zarling, and S.-L. Hu.** 1990. Human immunodeficiency virus-like, nonreplicating *gag-env* particles assemble in a recombinant vaccinia virus expression system. J. Virol. **64:**2653–2659.
23. **Hansen, M., L. Jelinek, S. Whiting, and E. Barklis.** 1990. Transport and assembly of *gag* proteins into Moloney murine leukemia virus. J. Virol. **64:**5306–5316.
24. **Harrison, G. P., and A. M. L. Lever.** 1992. The human immunodeficiency virus type 1 packaging signal and major splice donor region have a conserved stable secondary structure. J. Virol. **66:**4144–4153.
25. **Hayashi, T., T. Shioda, Y. Iwakura, and H. Shibuta.** 1992. RNA packaging signal of human immunodeficiency virus type 1. Virology **188:**590–599.
26. **Henderson, L. E., M. A. Bowers, R. C. Sowder II, S. A. Serabyn, D. G. Johnson, J. W. Bess, Jr., L. O. Arthur, D. K. Bryant, and C. Fenselau.** 1992. Gag proteins of the highly replicative MN strain of human immunodeficiency virus type 1: posttranslational modifications, proteolytic processing, and complete amino acid sequences. J. Virol. **66:**1856–1865.
27. **Hong, S. S., and P. Boulanger.** 1993. Assembly-defective point mutants of the human immunodeficiency virus type 1 Gag precursor phenotypically expressed in recombinant baculovirus-infected cells. J. Virol. **67:**2787–2798.
28. **Housset, V., H. De Rocquigny, B. Roques, and J.-L. Darlix.** 1993. Basic amino acids flanking the zinc finger of Moloney murine leukemia virus nucleocapsid protein NCp10 are critical for virus infectivity. J. Virol. **67:**2537–2545.
29. **Huang, M., J. M. Orenstein, M. A. Martin, and E. O. Freed.** 1995. $p6^{Gag}$ is required for particle production from full-length human immunodeficiency virus type 1 molecular clones expressing protease. J. Virol. **69:**6810–6818.
30. **Jacobson, R. H., and B. W. Matthews.** 1992. Crystallization of beta-galactosidase from Escherichia coli. J. Mol. Biol. **223:**1177–1182.
31. **Jentoft, J. E., L. M. Smith, X. Fu, M. Johnson, and J. Leis.** 1988. Conserved cysteine and histidine residues of the avian myeloblastosis virus nucleocapsid protein are essential for viral replication but not "zinc-binding fingers." Proc. Natl. Acad. Sci. USA **85:**7094–7098.
32. **Jones, T., G. Blaug, M. Hansen, and E. Barklis.** 1990. Assembly of Gag–β-galactosidase proteins into retrovirus particles. J. Virol. **64:**2265–2279.
33. **Jowett, J. M. B., D. J. Hockley, M. V. Nermut, and I. M. Jones.** 1992. Distinct signals in human immunodeficiency virus type 1 Pr55 necessary for RNA binding and particle formation. J. Gen. Virol. **73:**3079–3086.
34. **Kaplan, A. H., M. Manchester, and R. Swanstrom.** 1994. The activity of the protease of human immunodeficiency virus type 1 is initiated at the membrane of infected cells before the release of viral proteins and is required for release to occur with maximum efficiency. J. Virol. **68:**6782–6786.
35. **Karacostas, V., K. Nagashima, M. A. Gonda, and B. Moss.** 1989. Human immunodeficiency virus-like particles produced by a vaccinia virus expression vector. Proc. Natl. Acad. Sci. USA **86:**8964–8967.
36. **Katoh, I., Y. Yoshinaka, A. Rein, M. Shibuya, T. Odaka, and S. Oroszlan.** 1985. Murine leukemia virus maturation: protease region required for conversion from "immature" to "mature" core form and for virus infectivity. Virology **145:**280–292.
37. **Kaye, J. F., and A. M. Lever.** 1996. *trans*-acting proteins involved in RNA encapsidation and viral assembly in human immunodeficiency virus type 1. J. Virol. **70:**880–886.
38. **Krausslich, H. G., M. Facke, A. M. Heuser, J. Konvalinka, and H. Zentgraf.** 1995. The spacer peptide between human immunodeficiency virus capsid and nucleocapsid proteins is essential for ordered assembly and viral infectivity. J. Virol. **69:**3407–3419.
39. **Leis, J., D. Baltimore, J. B. Bishop, J. Coffin, E. Fleissner, S. P. Goff, S. Oroszlan, H. Robinson, A. M. Skalka, H. M. Temin, and V. Vogt.** 1988. Standardized and simplified nomenclature for proteins common to all retroviruses. J. Virol. **62:**1808–1809.
40. **Lever, A., H. Gottlinger, W. Haseltine, and J. Sodroski.** 1989. Identification of a sequence required for efficient packaging of human immunodeficiency virus type 1 RNA into virions. J. Virol. **63:**4085–4087.
41. **Luban, J., and S. P. Goff.** 1991. Binding of human immunodeficiency virus type 1 (HIV-1) RNA to recombinant HIV-1 *gag* polyprotein. J. Virol. **65:**3203–3212.
42. **McBride, M. S., and A. T. Panganiban.** 1996. The human immunodeficiency virus type 1 encapsidation site is a multipartite RNA element composed of functional hairpin structures. J. Virol. **70:**2963–2973.
43. **McDermott, J., L. Farrell, R. Ross, and E. Barklis.** 1996. Structural analysis of human immunodeficiency virus type 1 Gag protein interactions, using cysteine-specific reagents. J. Virol. **70:**5106–5114.
44. **Mergener, K., M. Facke, R. Welker, V. Brinkmann, H. R. Gelderblom, and H. G. Krausslich.** 1992. Analysis of HIV particle formation using transient expression of subviral constructs in mammalian cells. Virology **186:**25–39.
45. **Meric, C., and S. P. Goff.** 1989. Characterization of Moloney murine leukemia virus mutants with single-amino-acid substitutions in the Cys-His box of the nucleocapsid protein. J. Virol. **63:**1558–1568.
46. **Mervis, R. J., N. Ahmad, E. P. Lillehoj, M. G. Raum, F. H. R. Salazar, H. W. Chan, and S. Venkatesan.** 1988. The *gag* gene products of human immunodeficiency virus type 1: alignment within the *gag* open reading frame, identification of posttranslational modifications, and evidence for alternative *gag* precursors. J. Virol. **62:**3993–4002.
47. **Morellet, N., H. de Rocquigny, Y. Mely, N. Jullian, H. Demene, M. Ottmann, D. Gerard, J.-L. Darlix, M. C. Fournie-Zaluski, and B. P. Roques.** 1994. Conformational behaviour of the active and inactive forms of the nucleocapsid NCp7 of HIV-1 studied by ^{1}HNMR. J. Mol. Biol. **235:**287–301.
48. **Mulligan, R. C., and P. Berg.** 1981. Selection for animal cells that express the Escherichia coli gene coding for xanthine-guanine phosphoribosyltransferase. Proc. Natl. Acad. Sci. USA **78:**2072–2076.
49. **Otridge, J., and P. Gollnick.** 1993. MtrB from Bacillus subtilis binds specifically to trp leader RNA in a tryptophan-dependent manner. Proc. Natl. Acad. Sci. USA **90:**128–132.

50. **Ottmann, M., C. Gabus, and J.-L. Darlix.** 1995. The central globular domain of the nucleocapsid protein of human immunodeficiency virus type 1 is critical for virion structure and infectivity. J. Virol. **69:**1778–1784.
51. **Overton, H. A., Y. Fuji, I. R. Price, and I. M. Jones.** 1989. The protease and gag gene products of the human immunodeficiency virus: authentic cleavage and post-translational modification in an insect cell expression system. Virology **170:**107–116.
52. **Page, K. A., N. R. Landau, and D. R. Littman.** 1990. Construction and use of a human immunodeficiency virus vector for analysis of virus infectivity. J. Virol. **64:**5270–5276.
53. **Park, J., and C. D. Morrow.** 1992. The nonmyristylated Pr160$^{gag\text{-}pol}$ polyprotein of human immunodeficiency virus type 1 interacts with Pr55^{gag} and is incorporated into viruslike particles. J. Virol. **66:**6304–6313.
54. **Park, J., and C. D. Morrow.** 1993. Mutations in the protease gene of human immunodeficiency virus type 1 affect release and stability of virus particles. Virology **194:**843–850.
55. **Ratner, L., W. Haseltine, R. Patarca, K. J. Livak, B. Starcich, S. F. Josephs, E. R. Doran, J. A. Rafalski, E. A. Whitehorn, K. Baumeister, L. Ivanoff, S. R. Petteway, Jr., M. L. Pearson, J. A. Lautenberger, T. S. Papas, J. Ghrayeb, N. T. Chang, R. C. Gallo, and F. Wong-Staal.** 1985. Complete nucleotide sequences of the AIDS virus, HTLV-III. Nature **313:**277–284.
56. **Reik, W., H. Weiher, and R. Jaenisch.** 1985. Replication-competent M-MuLV carrying a bacterial suppresser tRNA gene: selective cloning of proviral and flanking host sequences. Proc. Natl. Acad. Sci. USA **82:**1141–1145.
57. **Sakaguchi, K., N. Zambrano, E. T. Baldwin, B. A. Shapiro, J. W. Erickson, J. G. Omichinske, G. M. Clore, A. M. Gronenborn, and E. Appella.** 1993. Identification of a binding site for the human immunodeficiency virus type 1 nucleocapsid protein. Proc. Natl. Acad. Sci. USA **90:**5219–5223.
58. **Shioda, T., and H. Shibuta.** 1990. Production of human immunodeficiency virus (HIV)-like particles from cells infected with recombinant vaccinia viruses carrying the gag gene of HIV. Virology **175:**139–148.
59. **Smith, A. J., M.-I. Cho, M.-L. Hammarskjöld, and D. Rekosh.** 1990. Human immunodeficiency virus type 1 Pr55^{Gag} and Pr160$^{gag\text{-}pol}$ expressed from a simian virus 40 late replacement vector are efficiently processed and assembled into viruslike particles. J. Virol. **64:**2743–2750.
60. **Smith, A. J., N. Srinivasakumar, M.-L. Hammarskjöld, and D. Rekosh.** 1993. Requirements for incorporation of Pr160$^{gag\text{-}pol}$ from human immunodeficiency virus type 1 into virus-like particles. J. Virol. **67:**2266–2275.
61. **Spearman, P., J.-J. Wang, N. V. Heyden, and L. Ratner.** 1994. Identification of human immunodeficiency virus type 1 Gag protein domains essential to membrane binding and particle assembly. J. Virol. **68:**3232–3242.
62. **Srinivasakumar, N., M. L. Hammarskjöld, and D. Rekosh.** 1995. Characterization of deletion mutations in the capsid region of human immunodeficiency virus type 1 that affect particle formation and Gag-Pol precursor incorporation. J. Virol. **69:**6106–6114.
63. **Stewart, L., G. Schatz, and V. Vogt.** 1990. Properties of avian retrovirus particles defective in viral protease. J. Virol. **64:**5076–5092.
64. **Summers, M. F., L. E. Henderson, M. R. Chance, J. W. Bess, Jr., T. L. South, P. R. Blake, I. Sagi, G. Peret Alvarado, R. C. Sowder III, D. R. Hare, and L. O. Arthur.** 1992. Nucleocapsid zinc finger detected in retroviruses: EXAFS studies of intact viruses and the solution-state structure of the nucleocapsid protein from HIV-1. Protein Sci. **1:**563–574.
65. **Wain-Hobson, S., P. Sonigo, O. Danos, S. Cole, and M. Alizon.** 1985. Nucleotide sequence of the AIDS virus, LAV. Cell **40:**9–17.
66. **Wang, C.-T., and E. Barklis.** 1993. Assembly, processing and infectivity of human immunodeficiency virus type 1 Gag mutants. J. Virol. **67:**4264–4273.
67. **Wang, C.-T., Y. Zhang, J. McDermott, and E. Barklis.** 1993. Conditional infectivity of a human immunodeficiency virus matrix domain deletion mutant. J. Virol. **67:**7067–7076.
68. **Wang, C.-T., J. Stegeman-Olsen, Y. Zhang, and E. Barklis.** 1994. Assembly of HIV Gag–β-galactosidase fusion proteins into virus particles. Virology **200:**524–534.
69. **Weldon, R., and J. Wills.** 1993. Characterization of a small (25-kilodalton) derivative of the Rous sarcoma virus Gag protein competent for particle release. J. Virol. **67:**5550–5561.
70. **Wills, J. W., C. E. Cameron, C. B. Wilson, Y. Xiang, R. P. Bennett, and J. Leis.** 1994. An assembly domain of the Rous sarcoma virus Gag protein required late in budding. J. Virol. **68:**6605–6618.
71. **Zhang, Y., and E. Barklis.** 1995. Nucleocapsid protein effects on the specificity of retrovirus RNA encapsidation. J. Virol. **69:**5716–5722.